

Time-Frequency Analysis of Time Localizable Linear Transform Based on DFT

Kook Yeon Kwak*

Richard A. Hadadd

Electrical Engineering Department
Polytechnic University
Six Metrotech Center Brooklyn, NY 11201, (e-mail) kkwakphoton.poly.edu

Abstract

A class of new orthonormal transforms, Time Localizable Linear Transform (TLLT), which is constructed from a traditional linear transform and gives the nonuniform time-frequency tiling was recently introduced by authors. Time Localizable DFT (TLDFDFT) is a subclass of TLLT constructed from DFT. In this paper, we are concerned with time-frequency characteristics of TLDFDFT bases to analyze qualitatively the performance of TLDFDFT in the time-frequency decomposition. Specially we investigate their phase characteristic since TLDFDFT bases concentrate their energies into the associated time locations and are inherently non-symmetric over the entire transform length.

1 Introduction

When we acquire a signal we can decompose it with some basis functions and calculate its associated coefficients with which we analyze the signal. There are many candidates as basis functions in the library of orthonormal transforms including *DFT*, *DCT*, Short Time Fourier Transform (*STFT*) and Wavelet Transform (*WT*). Conventional linear transforms like *DFT* and *DCT* are widely used with fast computational algorithms in signal processing and are adopted as standards like JPEG, MPEG1, and MPEG2 in signal coding but they do not properly represent time-localized signals. For the analysis of non-stationary signals, *STFT* has been used to decompose them over the time-frequency domain[1]. The *STFT* results in a uniform tiling of the time-frequency plane which imposes restrictions on analysis-performances. The

discrete *WT* (*DWT*) provides a non-uniform time-frequency tiling which can "zoom in" on signals with short bursts of high frequency[2][3]. But in implementing *DWT*, no innovative computational algorithm like *FFT* is found and the structure is totally different from that of transform in standards. Recently a family of the orthonormal transforms, the Time Localizable Linear Transform (*TLLT*) was proposed by authors[4]. The *TLLT* is a unitary transform with non-uniform time-frequency tiling property which is constructed from a Linear Transform with the fast algorithm. The *TLLT*'s are implemented by the fast algorithm and have compatibility with traditional linear transform at least in structure. The Time Localizable DFT (*TLDFDFT*) is a subclass of the *TLLT*, which is constructed on *DFT*.

In this paper, we investigate the time-frequency characteristics of *TLDFDFT* basis functions to analyze qualitatively the performance of *TLDFDFT* in the time-frequency decomposition. Specially we are concerned about phase characteristics in frequency domain to examine effects of asymmetric waveforms of *TLDFDFT* bases. We summarize *TLDFDFT* in succeeding subsections, derive time-frequency characteristics of *TLDFDFT* in section 2, demonstrate them by numerical calculation in section 3, and conclude finally.

1.1 Time Localizable Linear Transform

In constructing *TLLT*, we start with a $\ell^2(Z)$ space, S , spanned by the set of bases of a given linear transform. We partition S into orthogonal subspaces spanned by associated subsets of the given bases. And for each subspace, we find a set of new orthonormal bases by a linear combination of basis functions in the partitioned subset such that new basis functions concentrate their energies in certain time locations. Since subspaces are orthogonal, just the union of these new sets achieve the set of *TLLT* bases. Each lin-

*He is Ph.D. student in the Polytechnic University supported by GoldStar Co. in Korea that he is working for.

ear combination of the given bases can be represented by a matrix. A sufficient condition for new bases to be orthonormal is that the matrix in each subspace should be unitary. Furthermore each row sequence of these matrices should have the symmetry and periodicity properties for fast calculation. Our object is to find the optimal matrices satisfying the above two constraints and making the induced basis sequences concentrate the energy maximally in the corresponding location.

1.2 Time Localizable DFT (TLDFD)

With the DFT bases, solution of the optimization problem summarized as:

for the k -th subspace of dimension M_k spanned by the subset consisting of DFT bases consecutively in frequency index, matrix with element $a_{i,l}$ such that,

$$a_{i,l} = \frac{1}{\sqrt{M_k}} e^{-j \frac{2\pi}{M_k} (i+\alpha)l}, \quad (1)$$

where $\alpha = \frac{1}{2}(1 - \frac{M_k}{N})$, $0 \leq i, l \leq M_k - 1$, induces the subset of TLDFD bases concentrating energies maximally in the location of $[\frac{N}{M_k}i, \frac{N}{M_k}(i+1) - 1]$.

Supposed the space S has the dimension N and the k -th subspace are spanned by the set of DFT bases with the lowest frequency index k_0 . Then, $\psi_{k,i}$, a basis function in the TLDFD bases set spanning the subspace, is expressed:

$$\psi_{k,i}(n) = \sum_{l=0}^{M_k-1} a_{i,l} \frac{1}{\sqrt{N}} e^{j \frac{2\pi}{N} (k_0+l)n} \quad (2)$$

Clearly the matrix has IDFT structure. And TLDFD coefficients can be calculated by performing IDFT's of subsets of DFT coefficients. Fig.1 (a) and (b) show the position of TLDFD in the orthonormal transform space and an example of implementation of TLDFD, respectively.

2 Time-frequency analysis of TLDFD

A discrete transform has the time-frequency tiling consisting of cells where transform basis functions concentrate energies. The more energies are concentrated, the better time-frequency decomposition is achieved[6]. As the measure of the energy concentration, rms spread values of basis functions are popularly used.[6][5].

A basis sequence of TLDFD, $\psi_{k,i}(n)$, has two parameters k and i for indexing the subspace and the location

of energy concentration. These are similar to the scaling and shifting parameters respectively in the wavelet transform. Parameters, k and i , determine the location of the associated cell along the frequency and time axis.

2.1 Time characteristics of TLDFD bases

By performing the summation in the equation (2), we can easily express TLDFD basis functions as:

$$\psi_{k,i}(n) = \frac{1}{\sqrt{M_k N}} \frac{\sin \frac{\pi}{N} M_k (n - c_i)}{\sin \frac{\pi}{N} (n - c_i)} e^{j \frac{2\pi}{N} (k \cdot n - \Delta k c_i)} \quad (3)$$

for $0 \leq n \leq N-1$, where $c_i = \frac{N}{M_k}(i+\alpha)$, $k_c = k_0 + \Delta k$, and $\Delta k = \frac{M_k-1}{2}$. The c_i indicates the peak point of energy concentration of $\psi_{k,i}(n)$. From the Eqn. (3), we can observe some properties of TLDFD basis functions on the time domain. For any k ,

- the amplitude of the i -th TLDFD basis function is circularly right-shifted version of that of the $(i-1)$ -th basis function by $\frac{N}{M_k}$ points. And for the amplitude characteristic, it is enough to observe basis function of $i=0$.

- The amplitude of $\psi_{k,0}(n)$ is circularly symmetric with the center of c_i over the transform length N . Therefore, every basis function has the fully symmetric amplitude over the interval where its energy is concentrated. they cover the entire transform length making the total instantaneous energy at any point be constant.

- TLDFD basis functions have linear phase of the same slope $\frac{2\pi}{N} k_c$ in the time domain. This slope is the center frequency of the frequency band associated with k -th subspace in the arithmetic mean sense.

These observations show the fact that every TLDFD basis function is conjugate symmetric with constant phase shifting over the interval where its energy is concentrated. This suggests that the phase characteristic of the TLDFD basis function is nearly linear in the frequency band where energy is concentrated. This will be verified by the frequency characteristics in the following subsection.

Using the Eqn. (3) we can calculate the rms spread value of TLDFD basis functions,

$$\sigma_n^2 = \frac{1}{M_k N} \sum_{n=0}^{N-1} (n - \bar{n}_i)^2 \frac{\sin^2(\frac{\pi}{N} M_k (n - c_i))}{\sin^2(\frac{\pi}{N} (n - c_i))} \quad (4)$$

where $\bar{n}_i = \sum_n n |\psi_{k,i}(n)|^2$. It is not easy to express σ_n in the close form but it is easy to notice that σ_n is decreased as M_k is increased.

2.2 Frequency characteristics of $TLDFT$ bases

The Eqn. (3) shows that $TLDFT$ basis functions for the k -th subspace have modulation forms of basic functions with the center frequency of $\frac{2\pi}{N}k_c$. The basic functions are dependent of only the dimension of the subspace which is numbers of DFT bases combined to induce $TLDFT$ bases. For the subspace of dimension M_k , the basic functions are expressed:

$$\begin{aligned}\psi_{M_k;i}(n) &= \frac{1}{\sqrt{M_k N}} \frac{\sin(\frac{\pi}{N}M_k(n - c_i))}{\sin(\frac{\pi}{N}(n - c_i))} e^{-j\Delta k c_i} \quad (5) \\ &= \frac{1}{\sqrt{M_k N}} \sum_{l=0}^{M_k-1} e^{j\frac{2\pi}{N}((l-\Delta k)n - c_i l)} \quad (6)\end{aligned}$$

Frequency characteristics of $\psi_{M_k;i}(n)$ is obtained by shifting those of the basic function by $\frac{2\pi}{N}$ along the frequency axis.

$$\Psi_{M_k;i}(\omega) = \sum_{n=0}^{N-1} \psi_{M_k;i}(n) e^{-j\omega n} \quad (7)$$

$$= \frac{1}{\sqrt{M_k N}} \sum_{l=0}^{M_k-1} H_l(\omega) e^{-j\frac{2\pi}{N}c_i l} \quad (8)$$

where,

$$H_l(\omega) = \frac{\sin(\frac{N}{2}(\omega - \frac{2\pi}{N}(l - \Delta k)))}{\sin(\frac{1}{2}(\omega - \frac{2\pi}{N}(l - \Delta k)))} e^{-j(\frac{N-1}{2}(\omega - \frac{2\pi}{N}(l - \Delta k)))} \quad (9)$$

The Fourier transform, $\Psi_{M_k;i}(\omega)$, is calculated by the linear combination of M_k frequency functions, $H_l(\omega)$. Those functions are situated such that the distance between peak points of two adjacent functions is $\frac{2\pi}{N}$ and main lobes are located symmetrically around the DC. From this observation, we can expect that the $\Psi_{M_k;i}(\omega)$, has the amplitude characteristic of a low pass filter with the bandwidth $\frac{2\pi}{N}M_k$ and the frequency characteristic of $TLDFT$ basis has that of band pass filter that is the shifted version of this low pass filter by $\frac{2\pi}{N}k_c$. The k -th subspace represents roughly the frequency band of $\frac{k_0}{N}\pi \leq \omega \leq \frac{k_0 + M_k - 1}{N}\pi$. Its dimension, M_k , is associated with the bandwidth. The phase characteristic of the basic function in the frequency domain is somewhat complicated to be expressed in a closed form. But the function, $H_l(\omega)$ has values of zero at frequency points $\{\omega_j : \omega_j = \frac{2\pi}{N}(j - \Delta k), 0 \leq j \leq M_k - 1, j \neq l\}$ and has $\frac{N}{M_k} \mathcal{L}(-\frac{2\pi}{N}c_i l)$ at the frequency point, ω_l . Since the value of $\Psi_{M_k;i}(\omega)$ at ω_j is determined by only $H_j(\omega)$, if evaluating phases at only frequency points of $\{\omega_j : 0 \leq j \leq M_k - 1\}$,

$\Psi_{M_k;i}(\omega)$ has linear phase response of the slope, $-c_i$. This shows that the group delay function is fluctuated around c_i . This analysis is reasonable since $\psi_{M_k;i}(n)$ has the locally symmetric main lobe with the peak point at $n = c_i$. In the proximity of each ω_j , the slope of the phase function is $-\frac{(N-1)}{2}$. As the overall slope $-c_i$ approaches to this slope, so the phase response function approaches to the linear line. And we can expect that the phase response of the $TLDFT$ basis function in the frequency domain approaches to the linear phase as the peak point of its main lobe approaches to the half of transform length.

The rms spread value of the frequency characteristic function is calculated numerically:

$$\sigma_\omega^2 = \frac{1}{2\pi} \int_{-\pi}^{\pi} (\omega - \bar{\omega})^2 \left| \Psi_{M_k;i}(\omega - \frac{2\pi}{N}k_c) \right|^2 d\omega \quad (10)$$

where $\bar{\omega}$ is the center of mass of $\left| \Psi_{M_k;i}(\omega - \frac{2\pi}{N}k_c) \right|^2$.

2.3 Time-frequency tiling

In partitioning the space, we first determine center frequencies, $\frac{2\pi}{N}k_c$, and the bandwidths, $\frac{2\pi}{N}M_k$ of subspaces. With these data, we create the time-frequency tiling of the $TLDFT$ as:

- segment the time-frequency plane by horizontal bands associated with subspaces such that a band has the time length N , the frequency width of the associated subspace, and its vertical center at the center frequency,

- divide the horizontal band into M_k rectangular slots such that their horizontal centers are located at c_i , $0 \leq i \leq M_k - 1$. A slot in the time-frequency tiling is indicated by parameters k and i and has the dimension of N/M_k by $\frac{2\pi}{N}M_k$. Since c_i is a function of i and α , we have another parameter for tiling, α , determined independently in each subspace. By varying α , we shift the horizontal positions of slots circularly over the transform length within the band associated with a subspace. Some portion of the first or last slot is squeezed into the other side by circular shifting. With α , we can adjust slightly the time-frequency tiling as desired.

3 Numerical results

We calculate magnitudes and phases of $TLDFT$ basis functions in time and frequency domains for the visual display. Assuming that the transform length $N = 64$ and one of subspaces partitioned has the dimension 8 in this example. Since $TLDFT$ bases of a

subspace still hold features of time-frequency characteristics of whole *TLDF*T bases, we investigate just *TLDF*T bases of subspace with the dimension 8, the center frequency $(2\pi/N)(11.5)$, and $\alpha = 0.4375$. Fig. 2, 3, and 4 show the energy distribution in the time domain, the energy distribution in the frequency domain, and the phase characteristic in the frequency domain, respectively, of *TLDF*T bases with the energy concentrating location index $i = 0$ (dotted line) and $i = 1$ (dashed line). Fig. 5, 6, and 7 show the energy distribution in the time domain, the energy distribution in the frequency domain, and the phase characteristic in the frequency domain, respectively, of *TLDF*T bases with the energy concentrating location index $i = 2$ (dotted line) and $i = 3$ (dashed line). Table 1 shows rms spread values σ_n and σ_ω of these *TLDF*T basis functions. For $i = 0$, rms spread value in the time domain is somewhat large because of parts of the main lobe spilled over the far other side.

4 conclusions

Fig. 3 and 6 show that *TLDF*T basis function is locally symmetrical over the energy concentration interval and Fig. 5 and 8 show the phase characteristic in the energy concentration frequency band is approximately linear. A partitioning of the space S results in a set of *TLDF*T bases. Since many partitionings are possible, *TLDF*T forms a family of orthonormal transforms. Each *TLDF*T has its own time-frequency tiling and *TLDF*T provides a family of abundant time-frequency tilings. Furthermore, *TLDF*T has much flexible time-frequency tiling due to the parameter, α , adjusting the peak point of energy concentration. And *TLDF*T can be implemented fast by *FFT* algorithms. We expect that *TLDF*T can be an excellent tool to represent a signal in time-frequency decomposition.

References

- [1] M. R. Portnoff, "Time-Frequency Representation of Digital Signals and Systems Based on the Short-Time Fourier Analysis," *IEEE Trans. on ASSP*, Vol. 28, pp. 55-69, Feb. 1980.
- [2] I. Daubechies, "Orthonormal Bases of Compactly Supported Wavelets," *Comm. in Pure and Applied Math.*, Vol. 41, pp. 909-996, 1988.
- [3] S. Mallat, "A Theory for Multiresolution Signal Decomposition: the Wavelet Representation,"

IEEE Trans. on Pattern Anal. and Mach. Intell., Vol. 11, pp. 674-693, Jul. 1989.

- [4] K. Y. Kwak, R.A. Haddad, "New family of orthonormal transforms with time localizability based on DFT," *Proc. of SPIE (VCIP conference '94)*, Vol.2308, pp. 1158-1169, 1994.
- [5] L. Cohen, "Time-Frequency Distributions-A Review," *Proc. of IEEE*, Vol.77, No. 7, pp. 941-981, Jul. 1989.
- [6] R. A. Haddad, A. N. Akansu, and A. Benyassine, "Time-frequency localization in transforms, subbands, and wavelets: a critical review," *Opt. Eng.*, Vol. 32, No. 7, pp 1411-1428, Jul. 1993.

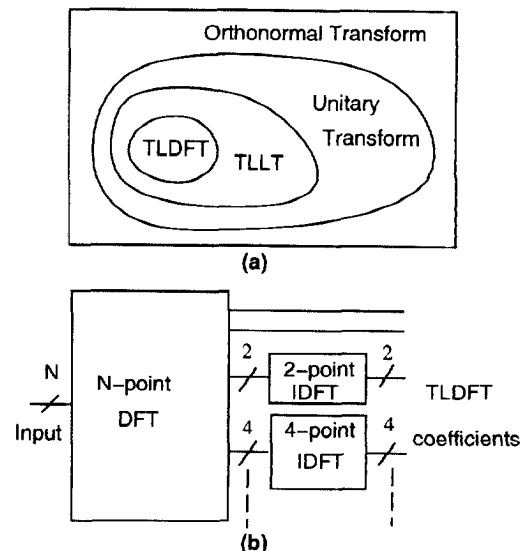


Figure 1: (a)Position of *TLDF*T in the orthonormal transform space, and (b) an example of implementation of *TLDF*T.

i	0	1	2	3
\bar{n}	10.59	13.45	20.36	27.76
$\bar{\omega}$	1.10	1.12	1.13	1.13
σ_n	17.32	8.95	6.82	6.09
σ_ω	0.48	0.27	0.25	0.24
$\sigma_n\sigma_\omega$	8.30	2.42	1.68	1.46

Table 1: rms spread values of *TLDF*T.

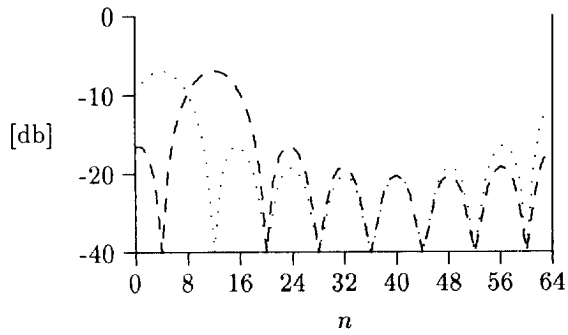


Figure 2: The energy distribution in time domain of *TLDF* bases with the energy concentration in the first(dotted) and the second(dashed) interval

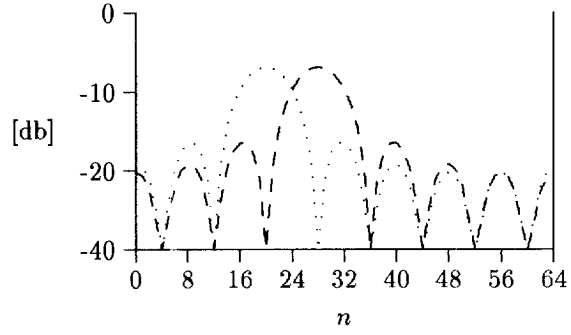


Figure 5: The energy distribution in time domain of *TLDF* bases with the energy concentration in the third(dotted) and the fourth(dashed) interval

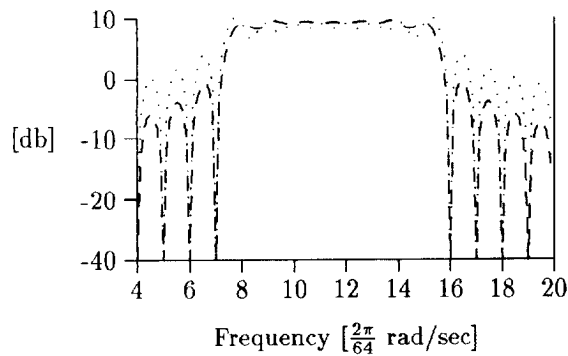


Figure 3: The energy distribution in frequency domain of *TLDF* bases with the energy concentration in the first(dotted) and the second(dashed) interval

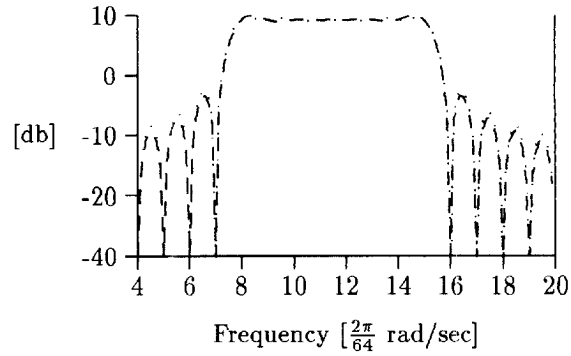


Figure 6: The energy distribution in frequency domain of *TLDF* bases with the energy concentration in the third(dotted) and the fourth(dashed) interval

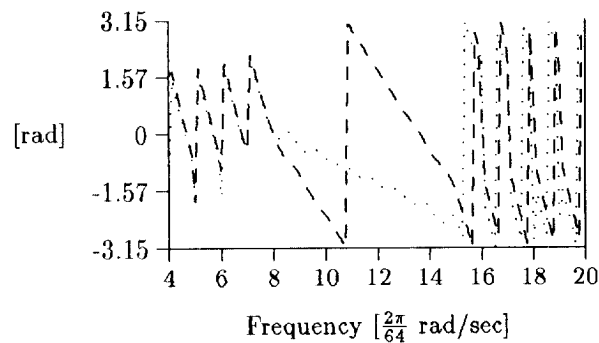


Figure 4: The phase characteristic in frequency domain of *TLDF* bases with the energy concentration in the first(dotted) and the second(dashed) interval

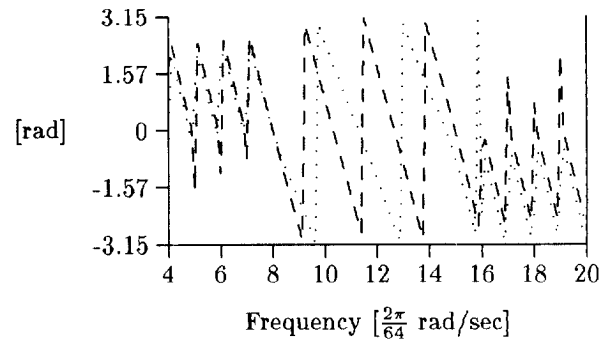


Figure 7: The phase characteristic in frequency domain of *TLDF* bases with the energy concentration in the third(dotted) and the fourth(dashed) interval